loss is very high, and, because of the fourth-power relation of the temperature, it falls off rapidly at lower temperatures.

The liquidus temperature of the synthetic lunar sample is somewhat higher than that of basalts, and, if the flow is extruded at or near this temperature, the radiant heat loss from the surface would be very large. A solid crust will form quickly, and the surface temperature will subsequently be governed by the rate of conduction from the molten interior. If we assume that the thermal diffusivity does not differ radically from that of other silicates, the heat loss will be greatly reduced by the insulating effect of the crust and the lava will remain fluid in its interior.

These relations favor the formation of lava tubes. On the moon the tubes will be broader than they are on the earth because of the higher stability of the roof in a low-gravity field and much longer because of the extreme fluidity of the liquid. It seems unlikely that the fluid part of a flow would be exposed except very close to the vent or for short times after the crust of a flow was ruptured.

Finally, the low viscosity implies high diffusion coefficients that would be consistent with the coarse crystallinity of the Apollo 11 samples. Even in our relatively rapid cooling of laboratory melts, crystals over a centimeter long were commonly formed, and complete crystallization occurred in samples that were cooled from 1450° to 1200°C in about 30 minutes.

TSUTOMU MURASE
ALEXANDER R. MCBIRNEY
Center for Volcanology, University of Oregon, Eugene 97403

References and Notes

1. Lunar Sample Preliminary Examination Team, *Science* **165**, 1211 (1969).
2. L. Shartsis and S. Spinner, *J. Res. Nat. Bur. Stand.* **46**, 176 (1951).
3. W. Eitel, *Silicate Science* (Academic Press, New York, 1965), vol. 2, p. 605.
4. T. Murase, *J. Fac. Sci. Hokkaido Univ. Ser. VII* **1**, 489 (1962). Revision of figure II-4 on the basis of new viscosity data derived from slags and rocks predicts that the viscosity of the synthetic lunar sample should be about 2 to 4 poises at 1500°C and 8 to 12 poises at 1400°C.
5. N. V. Zaimskikh and O. A. Esin, *Zh. Prikladnoi Khim.* **26**, 70 (1953).
6. Based on measured densities of the synthetic lunar sample at 1400°C and a Columbia River basalt at 1200°C.
7. This work was made possible by NASA research grant No. NGR 38-003-012.

26 November 1969; revised 2 January 1970 ■

Supersaturation of Gases in Water: Absence of Cavitation on Decompression from High Pressures

Abstract. *Very high supersaturations ranging from 140 atmospheres for oxygen to more than 270 atmospheres for helium, were produced without cavitation of the water at atmospheric pressure. Thus, the lower limits for* de novo *bubble formation are increased substantially over those previously obtained.*

Bubbles normally appear when water which has been saturated with gas at a few atmospheres pressure is exposed to atmospheric pressure. Such cavitation usually is initiated by minute gas nuclei present prior to the decompression. The supersaturation at which *de novo* bubble formation occurs is not known, although it is of general interest (*1*) and has practical implications for human diving. For instance, knowing the susceptibility to cavitation for various gases would aid in developing better gas mixtures and decompression procedures (*2*).

With the present simple technique, strikingly high supersaturations without cavitation have been obtained for various gases in water. Figure 1 shows the apparatus. After trapped air was expelled from the acid-cleaned capillary observation tube through the seal *a*, gas pressure was applied and the distilled water in cup *b* was equilibrated with the gas by shaking the assembly for 45 minutes. Tests showed this time to be more than twice that needed for complete equilibration. An inherent advantage of this method is that most of the cavitation nuclei, that is, small gas pockets, dissolve when the pressure is applied initially. After equilibration, the water saturated with gas was transferred under pressure to the capillary by slowly bleeding out water at seal *a*. The assembly was then turned to the horizontal position, and the pressure in it was lowered to ambient pressure within a few seconds while the water in the capillary was observed. When no bubbles had appeared after 10 minutes, the result was recorded as "no cavitation." Bubbles rarely appeared after this initial time period. When massive cavitation occurred, it sometimes started even before the pressure was released completely.

None of the gases tested cavitated the water at supersaturations less than 130 atm. At various pressures above this value, cavitation occurred with all gases except helium, which yielded no bubbles at pressures up to 270 atm (*3*). For each of the gases, there was a gradual increase in the number of bubbles appearing as the saturation pressure was increased. Instant, massive cavitation occurred only 10 to 20 atm above the highest supersaturations without cavitation. Examination of closeup movies showed that, during light and moderate cavitation, the bubbles always appeared to form at the glass-water interface. During massive cavitation, most of the bubbles appeared at the interface; however, there were indications that some bubbles also spontaneously appeared in the water. The results (Table 1) show that maximum supersaturations without cavitation occur at different pres-

Table 1. Supersaturation of gases in water at 25°C. In column 3 the lower of the two values is the saturation pressure which usually (two out of three trials) yielded no cavitation; the higher value is the highest observed saturation without cavitation. Column 5 lists gas solubility in water at 25°C and 1 atm (*7*). Each set of pressure values is based on 12 or more determinations near the point of cavitation made with several different samples of capillaries, distilled water, and gas.

Gas	Inner diameter (mm)	Maximum supersaturation without cavitation (atm)	Saturation for beginning massive cavitation (atm)	Gas solubility (cm³/cm³ water)
Argon	1.1	135–140	160	0.03123
Oxygen	1.1	135–140	155	.02830
Nitrogen	1.1	170–185	200	.01434
Helium	1.1	> 270	> 270	.00865
Nitrogen	2.5	145–155	170	
Nitrogen	0.6	170–190	205	
Nitrogen	0.4	165–190	210	
Nitrogen	0.15	160–170	195	

sures for each of the gases. Also, high supersaturations without cavitation were not dependent on confinement of the water in capillaries of small dimensions, such as is necessary for avoiding cavitation in water under tensile stress (*4*); there was little change in the cavitation properties when capillaries of dimensions ranging from 0.15 to 2.5 mm in inner diameter were used.

Since experimental reproducibility was excellent with different samples of glass, water, and gas, and since the pressure range from the condition of no cavitation to the beginning of massive cavitation was small and rather well defined for each of the gases, the pressures for beginning massive cavitation (Table 1, column 4) may represent the approximate value for *de novo* bubble formation at the water-gas interface and, possibly, also in the water body. The highest supersaturations without any cavitation (Table 1, column 3) represent the lowest possible limits for such bubble formation. The highest such value that had been obtained previously was 70 atm for nitrogen (*5*).

Since the pressure for bubble formation increases with decreasing gas solubility, the gas concentration rather than the pressure (that is, tension) appears to be the determining factor. In view of this, Haldane's classical maximum supersaturation limit for avoiding the "bends" (*6*) should be examined and possibly modified for gases other than nitrogen.

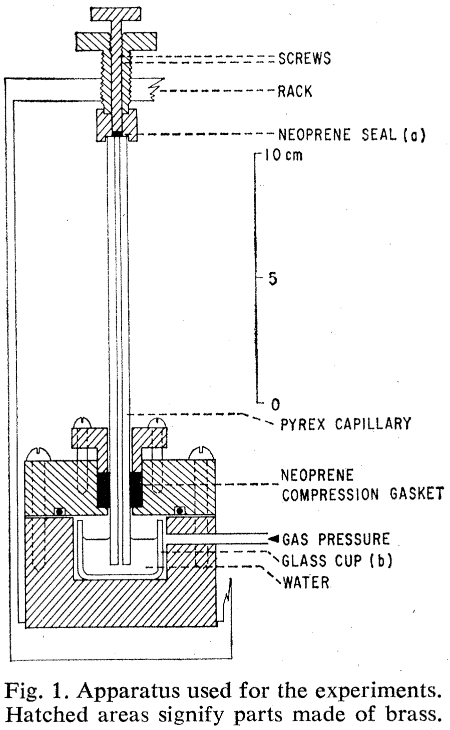

Fig. 1. Apparatus used for the experiments. Hatched areas signify parts made of brass.

E. A. Hemmingsen
*Physiological Research Laboratory,
Scripps Institution of Oceanography,
University of California at San Diego,
La Jolla 92037*

References and Notes

1. R. B. Dean, *J. Appl. Phys.* **15**, 446 (1944); E. N. Harvey, D. K. Barnes, W. D. McElroy, A. H. Whiteley, D. C. Pease, K. W. Cooper, *J. Cell. Comp. Physiol.* **24**, 1 (1944).
2. Recent reviews of this field can be found in *The Physiology and Medicine of Diving and Compressed Air Work*, P. B. Bennett and D. H. Elliot, Eds. (Baillière Tindall & Cassell, London, 1969), and in *Underwater Physiology*, C. J. Lambertsen, Ed. (Williams & Wilkins, Baltimore, 1967).
3. This was the highest value obtained before breakage of the capillary tubes. Because explosive breakage sometimes occurred at lower pressures as well, care must be taken during the experiments.
4. L. J. Briggs, *J. Appl. Phys.* **21**, 721 (1950).
5. F. B. Kenrick, K. L. Wismer, K. S. Wyatt, *J. Phys. Chem.* **28**, 1308 (1924).
6. With nitrogen as the main gas, in vivo bubbles are avoided by maintaining a ratio of supersaturation tension to external pressure of approximately 2 : 1, or less [J. S. Haldane and J. G. Priestley, *Respiration* (Yale Univ. Press, New Haven, 1935), pp. 327–362]. Most decompression procedures have made use of this ratio (see references in *2*).
7. E. Douglas, *J. Phys. Chem.* **68**, 169 (1964); R. F. Weiss, personal communication.
8. Supported by grant GM 10521 from the Department of Health, Education, and Welfare.

13 November 1969; revised 12 January 1970 ■

Uranium Localization on Hydroxyapatite by Analysis of Fission Fragment Tracks

Abstract. *The distribution of enriched uranium on individual hydroxyapatite crystals after an exchange reaction has been investigated by means of thermal neutron irradiation followed by electron microscopic analysis of fission fragment tracks in plastic support films. One uranyl ion for every two to three surface calcium ions became associated with the mineral but in a nonuniform distribution that strongly favors crystal end regions.*

Induced fission of uranium-235 in thin films has been shown to produce damage tracks in the films along the path of the ejected high-energy fission fragments (*1–3*). This physical process was first proposed as the basis of a high-resolution biological tracer system by Malmon (*4*), who also experimentally demonstrated the feasibility of the technique. In this report I describe the application of this new tracer technique to uranyl ion–hydroxyapatite exchange experiments. Because the experimental results could not have been obtained with other high-resolution tracer methods presently in use, a detailed comparison is included between the characteristics of the new system and other tracer techniques.

All high-resolution biological tracer systems in use at present are based upon (i) specific histochemical precipitation reactions, or (ii) immunochemical reactions that use an electron-dense tag on one component, or (iii) electron microscopic radioautography. All these basic processes are subject to numerous influences that can produce positive or negative artifacts, alter response threshold and sensitivity capabilities, and lead to nonuniform results from one area to another in a single sample (*5*). Also dissolution or loss of a precipitate (*6*) or latent image (*7*) can occur, diffusion can cause movement of established markers from their original position (*8*), and accurate quantitation of final results is difficult or impossible.

Maximum resolution capabilities of histochemical and immunochemical methods are limited by the minimum size of the precipitate or the electron-dense tag formed to areas of the order of 30 to 150 Å in diameter; resolution limits of electron microscopic radioautography are probability circles of 1000 to 3000 Å diameter or more (*9*).

Most of the deficiencies mentioned which are inherent in the above techniques cannot occur in the new system. The cumulative dose of thermal neutrons given the samples completely determines the fraction of uranium atoms that will undergo fission wherever they are located (*10*). Essentially all the fission events produce damages to thin plastic films with a relatively constant proportion of these having the configuration of tracks (*2, 4*). Accordingly, the sensitivity of the system is uniform in all areas of a sample and dose-controllable, and reasonably good quantitative estimations of the uranium content can be made from the numbers of tracks observed